Supporting Information

Materials and Methods

Experiment

In this study, an alloy IR probe which allowed us to get access to spectral windows of 2000–650 cm^{-1} at a resolution of 4 cm^{-1}, was inserted vertically down into a round-bottom flask in microwave reactor (**Scheme 1**) to interface with a scientific microwave unit. In order to ensure the safety and feasibility of the experiment, three potential problems might be induced by insertion of the probe directly into the reaction mixture were considered before the experiment. The first was that the probe could act as an antenna drawing microwave irradiation out of the cavity into the environment around the user. We set up the apparatus and used it to heat water and used a detector to monitor microwave leakage. We found that microwave leakage was below the Food and Drug Administration mandated limit for household microwave ovens of 5 mW cm^{-1} at 5 cm from the oven surface mainly because water is a high microwave absorbing substrate. Linked to the first problem, the second problem could be that a build-up of charge on the probe could occur during a run. We envisaged that the latter issue could be resolved by grounding the probe with a wire to link the probe to the attenuator of the microwave unit. The third problem was that alloy IR probe might be heated or interfered by microwave irradiation. Since the ReactIR probe was also equipped with a temperature measurement device at the tip, we texted the probe temperature during the microwave irradiation and found that the temperature of the ReactIR probe was very close ($\pm$ 2^{o}C) to the temperature of microwave reactor which was monitored by the Teflon platinum resistance temperature transducer. Furthermore, the ReactIR probe of FTIR spectrum was not found to be interfered by microwave irradiation since the wavelengths of infrared light (2.5 μm - 25 μm) used are much shorter than microwaves (1.25×10^{8} μm).

Scheme 1. ReactIR system interfaced with a scientific microwave unit.

Experiments were carried out following two different protocols: the effect of temperature on BSA conformation changes was conducted by increasing the temperatures from 20 to 70°C at 10°C interval under microwave heating and conventional heating (in EasyMax™ reactor), respectively; The effect of microwave power on BSA conformation changes was conducted by increasing the temperature from 20 to 60°C at different microwave power (160 W, 320 W, 480 W, 640 W and 800 W).

FTIR Spectrometer

In situ FTIR experiments were conducted at preset temperature by using Mettler Toledo ReactIR™ 15 equipped with a liquid nitrogen cooled MCT detector and with a diamond composite alloy Attenuated total reflectance (ATR) probe. The probe has a usable wavenumber range of 2000–650 cm^{-1} During the measurement, the probe was inserted inside of a scientific microwave unit (MCR 3), and immersed into the protein solution in a three neck round flask. BSA was used as a protein model since it is inexpensive, easily available, stability and well-characterized structure. Furthermore, several spectroscopic observables in the same protein have been reported. The BSA (from Shanghai Shenggong company, 98% purity, defatted) concentration used was 0.05 mM in pH 7.0 deionized water. FTIR spectra were measured at a spectral resolution of 4 cm^{-1} by accumulating 1024 scans.

FTIR spectroscopy analysis

Although the artifact problem is annoying in FTIR analysis, many advantages of FTIR make it a powerful tool in elucidating the secondary structure of protein and providing information on protein conformational changes (B. C. Smith, *Fundamentals of Fourier Transform Infrared Spectroscopy*, Second Edition, CRC Press, Boca Raton, FL, USA, 2011, pp. 207). High sensitivity to small variations in molecular geometry and hydrogen bonding patterns make the amide I (1700−1600 cm^{-1}) band uniquely useful for the analysis of protein secondary structural composition and conformational changes. In this study, amide I region was focused on to analyze secondary structure of BSA. It is well known that water adsorption has great effect on the amide I bands analysis of the protein since the amide I mode of proteins absorbs between 1600 cm^{-1} and 1700 cm^{-1}, overlapping directly with the H_2O bending vibrational mode at 1640 cm^{-1}. The contribution of water in the protein spectrum can be eliminated using digital subtraction by measuring water and the protein in water at identical conditions (D. M. Byler and H. Susi, *Biopolymer*, 1986, **25**, 469; A. Bouhekka and T. Bürgi, *Appl. Surf. Sci*., 2012, **261**, 369). In order to eliminate water adsorption in the amide I bands, the water absorption was subtracted from the spectra by measuring water and the BSA in water at identical conditions. A straight baseline of the subtraction spectra was obtained from 2000 to 1750 cm^{-1} which suggested the successfulness of water subtraction lead to higher quality protein spectra (J. C. Gorgat et al., *Proc. Nati. Acad. Sci. USA Immunology*, 1989, **86**, 2321; A. Dong et al., Biochem. 1992, **31**, 182–189). Notably, the observed amide I band contours of proteins or polypeptides consist of overlapping component bands, representing α-helices, β-sheets, turns and random structures, which lie in close proximity to one another and are instrumentally unresolvable. Second derivative analysis and curve fitting are the mostly popularly used methods to estimate quantitatively the relative contributions of different types of secondary structures in proteins from their IR amide I spectra (J. Kong and S. Yu, *Acta. Biochim. Biophys. Sin (Shanghai)*, 2007, **39**, 549). Therefore, assignments of the amide I band component to each secondary structure element were conducted by using second derivative analysis. A curve fitting procedure was used to calculate quantitatively the area of each component representing a type of secondary structure.

Second derivative of the FTIR spectrum of amide I region for secondary structure was analyzed by PEAKFIT software (version 4.12, Seasolve Software Inc., San Jose, Calif.) which has been successfully used in analysis of FTIR spectra of many proteins (G. S. T. Smith, et al. *Amino Acids*, 2010, **39**, 739; L. N. Rahman, et al. *Amino Acids*, 2011. **40**, 1485). The number and the location of peaks of the secondary structure components were verified by the second derivative of the baseline-corrected spectra of the BSA by using the AutoFit peaks II secondary derivative function. The parameters were left free to adjust iteratively, with the only restriction on the peak wavenumbers being to vary within a range of ± 2 cm^{-1} according to the reference (A Natalello et al, *Biochem J.* 2005, **385**, 511). The observed amide I bands of proteins thus consisted of overlapping secondary structure component bands. Auto-fits of the second derivative spectra of the original spectra were performed until the coefficient of determination (r^2) was larger than 0.99, and the bandwidths of the secondary structure components were < 20 cm^{-1}. The integrated areas derived from the curve-fitting analyses were used in calculating the various conformational states assigned to individual bands. Band assignment of BSA in the amide I region was according to the literatures (Bands between 1653 cm^{-1} and 1658 cm^{-1} are assigned to α-helix; bands between 1640 cm^{-1} and 1650 cm^{-1} are assigned to random coil; bands between 1662 cm^{-1} and 1681 cm^{-1} are assigned to β-turn and bands from 1685 cm^{-1} to 1696 cm^{-1} and from 1620 cm^{-1} to 1635 cm^{-1} are assigned to β-sheet). All FTIR experiments were performed in duplicate, and reproducible data were obtained. Detailed predictions of the proportions of different types of secondary structures (α-helix, β-strand, β-sheet, and random coil) are given in the Appendix.

Microwave equipment

Detections were carried out in a commercial multimode microwave reactor (MCR-3, Shanghai JieSi Microwave Chemistry Corporation). The machine consisted of a continuous focused microwave power delivery system with an operator selectable power output from 0 to 800 W. The temperature of the protein solution was monitored and kept constant (± 1^{o}C) by using a contact Teflon platinum resistance temperature transducer inserted directly into the protein solution.

Appendix

20^{o}C

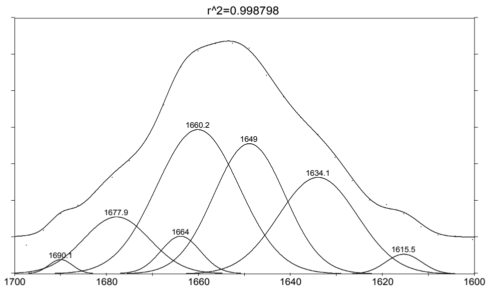

30^{o}C

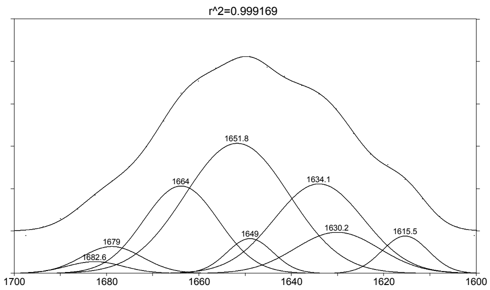

40^{o}C

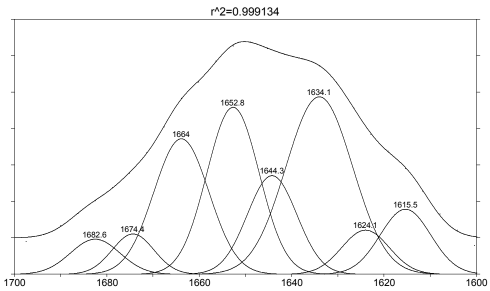

50^{o}C

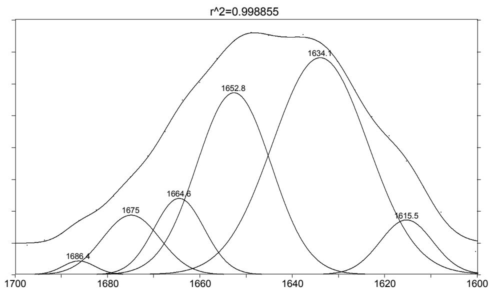

60^{o}C

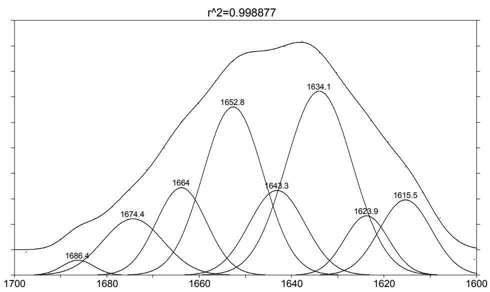

70^{o}C

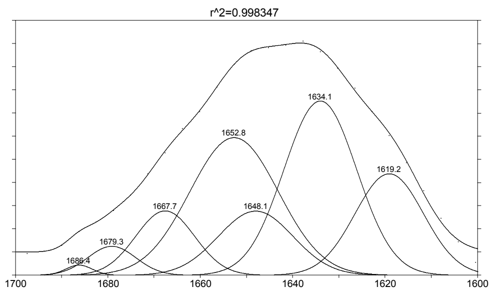

Figure A1. Secondary derivative FTIR spectrum under microwave irradiation in the temperature range of 20 to 70^{o}C.

Table A1. Infrared band positions, band areas determined by curve fitting, and band assignments in the amide I spectral region of BSA under microwave irradiation at different temperatures.

Sample	Band position (cm^{-1})	Percentage of band area (%)	Band Assignment
20°C	1615	2.0 ± 0.05	β-Sheet
	1634	21.7 ± 0.6	β-Sheet
	1649	26.4 ± 0.8	Random coil
	1660	33.9 ± 1.2	α-Helix
	1663	4.2 ± 0.1	β-Turn
	1677	10.7 ± 0.3	β-Turn
	1690	0.9 ± 0.08	β-Turn
30°C	1615	4.7 ± 0.1	β-Sheet
	1630	9.3 ± 0.1	β-Sheet
	1634	21.5 ± 0.3	β-Sheet
	1649	4.3 ± 0.07	Random coil
	1652	36.4 ± 1.3	α-Helix
	1664	17.6 ± 0.7	β-Turn
	1679	4.4 ± 0.1	β-Turn
	1683	1.8 ± 0.004	β-Turn
40°C	1616	7.9 ± 0.1	β-Sheet
	1624	5.0 ± 0.07	β-Sheet
	1634	28.4 ± 0.4	β-Sheet
	1644	11.7 ± 0.3	Random coil
	1653	20.9 ± 0.8	α-Helix
	1664	17.9 ± 0.2	β-Turn
	1674	4.0 ± 0.05	β-Turn
	1683	4.2 ± 0.06	β-Turn
50°C	1616	6.4 ± 0.07	β-Sheet
	1634	46.1 ± 0.7	β-Sheet
	1653	30.2 ± 0.9	α-Helix
	1665	8.6 ± 0.2	β-Turn
	1675	7.7 ± 0.1	β-Turn
	1686	1.0 ± 0.004	β-Turn
60°C	1616	9.4 ± 0.1	β-Sheet
	1624	6.3 ± 0.1	β-Sheet
	1634	29.1 ± 0.6	β-Sheet
	1643	11.3 ± 0.4	Random coil
	1653	24.1 ± 0.9	α-Helix
	1664	10.5 ± 0.2	β-Turn
	1674	8.1 ± 0.1	β-Turn
	1686	1.1 ± 0.006	β-Turn

70°C	1619	16.5 ± 0.7	β-Sheet
	1634	30.2 ± 1.0	β-Sheet
	1648	11.4 ± 0.2	Random coil
	1653	29.0 ± 1.0	α-Helix
	1668	9.0 ± 0.2	β-Turn
	1679	3.3 ± 0.008	β-Turn
	1686	0.6 ± 0.005	β-Turn

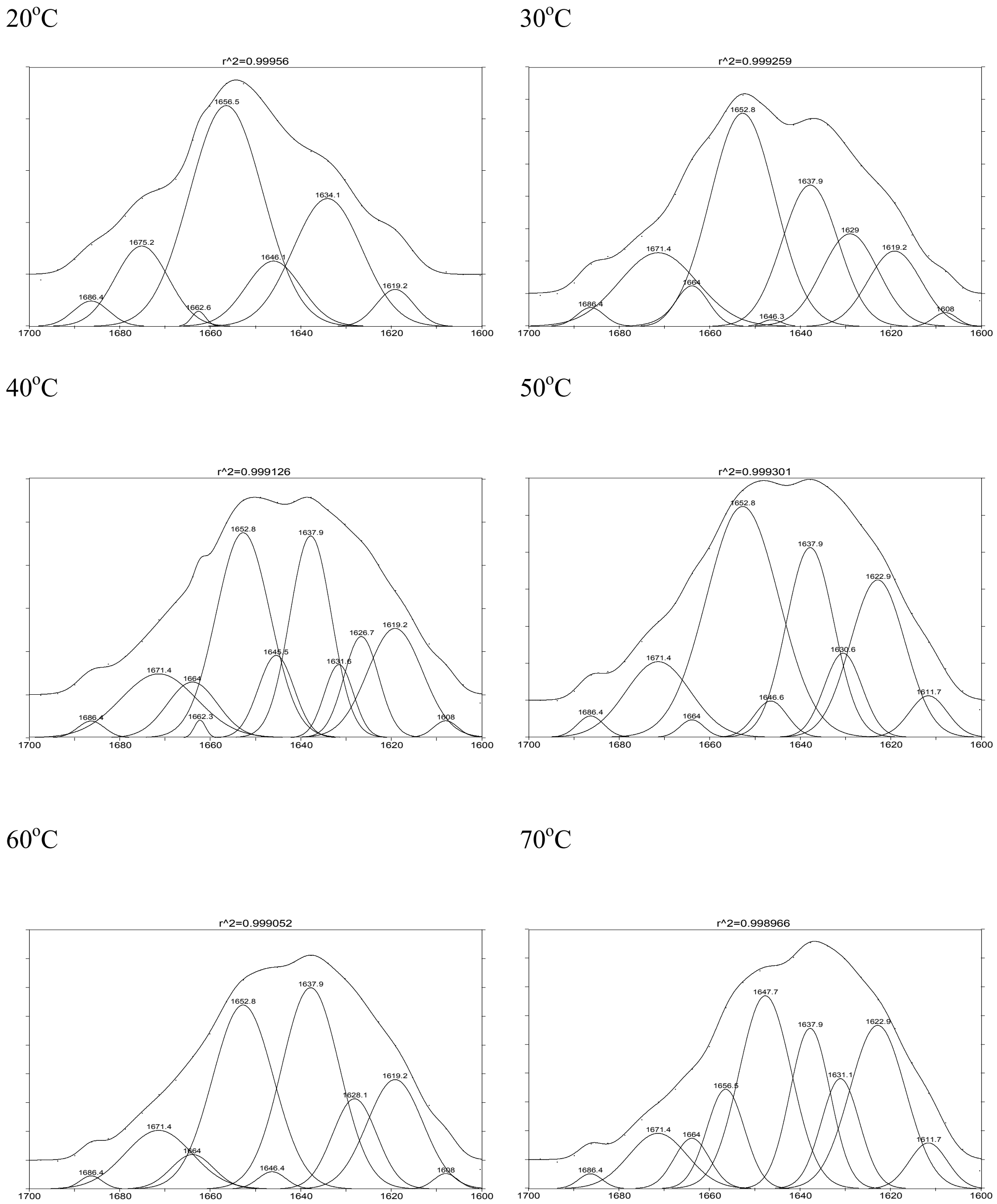

Figure A2. Secondary derivative FTIR spectrum under conventional heating in the temperature range of 20 to 70°C.

Table A2. Infrared band positions, band areas determined by curve fitting, and band assignments in the amide I spectral region of BSA under conventional heating at different temperatures.

Sample	Band position (cm^{-1})	Percentage of band area (%)	Band Assignment
20°C	1619	3.9 ± 0.2	β-Sheet
	1634	24.9 ± 0.5	β-Sheet
	1646	10.2 ± 0.3	Random coil
	1657	45.8 ± 2.1	α-Helix
	1663	0.6 ± 0.002	β-Turn
	1675	12.1 ± 0.4	β-Turn
	1686	2.5 ± 0.005	β-Turn
30°C	1608	0.9 ± 0.003	β-Sheet
	1619	10.3 ± 0.1	β-Sheet
	1629	13.3 ± 0.2	β-Sheet
	1638	20.3 ± 0.4	β-Sheet
	1646	0.3 ± 0.01	Random coil
	1653	35.4 ± 1.7	α-Helix
	1664	3.4 ± 0.1	β-Turn
	1671	14.6 ± 0.5	β-Turn
	1686	1.3 ± 0.005	β-Turn
40°C	1608	0.9 ± 0.04	β-Sheet
	1619	14.0 ± 0.3	β-Sheet
	1627	8.2 ± 0.2	β-Sheet
	1632	5.0 ± 0.2	β-Sheet
	1638	19.6 ± 0.3	β-Sheet
	1645	6.9 ± 0.06	Random coil
	1653	25.9 ± 1.1	α-Helix
	1662	0.5 ± 0.006	β-Turn
	1664	6.5 ± 0.1	β-Turn
	1671	11.4 ± 0.3	β-Turn
	1686	1.0 ± 0.004	β-Turn
50°C	1612	3.4 ± 0.08	β-Sheet
	1623	18.6 ± 0.5	β-Sheet
	1631	6.9 ± 0.2	β-Sheet
	1638	19.6 ± 0.3	β-Sheet
	1647	2.6 ± 0.09	Random coil
	1653	36.3 ± 1.8	α-Helix
	1664	0.9 ± 0.003	β-Turn
	1671	10.6 ± 0.1	β-Turn
	1686	1.2 ± 0.1	β-Turn
60°C	1608	0.9 ± 0.1	β-Sheet

	1619	15.5 ± 0.1	β-Sheet
	1628	10.1 ± 0.2	β-Sheet
	1638	29.5 ± 0.8	β-Sheet
	1646	1.2 ± 0.05	Random coil
	1653	28.4 ± 1.4	α-Helix
	1664	3.7 ± 0.1	β-Turn
	1671	9.9 ± 0.1	β-Turn
	1686	0.7 ± 0.005	β-Turn
70°C	1612	4.3 ± 0.009	β-Sheet
	1623	22.4 ± 0.5	β-Sheet
	1631	10.3 ± 0.1	β-Sheet
	1638	15.8 ± 0.3	β-Sheet
	1648	24.8 ± 0.9	Random coil
	1657	9.2 ± 0.5	α-Helix
	1664	4.4 ± 0.2	β-Turn
	1671	7.9 ± 0.1	β-Turn
	1686	0.9 ± 0.006	β-Turn

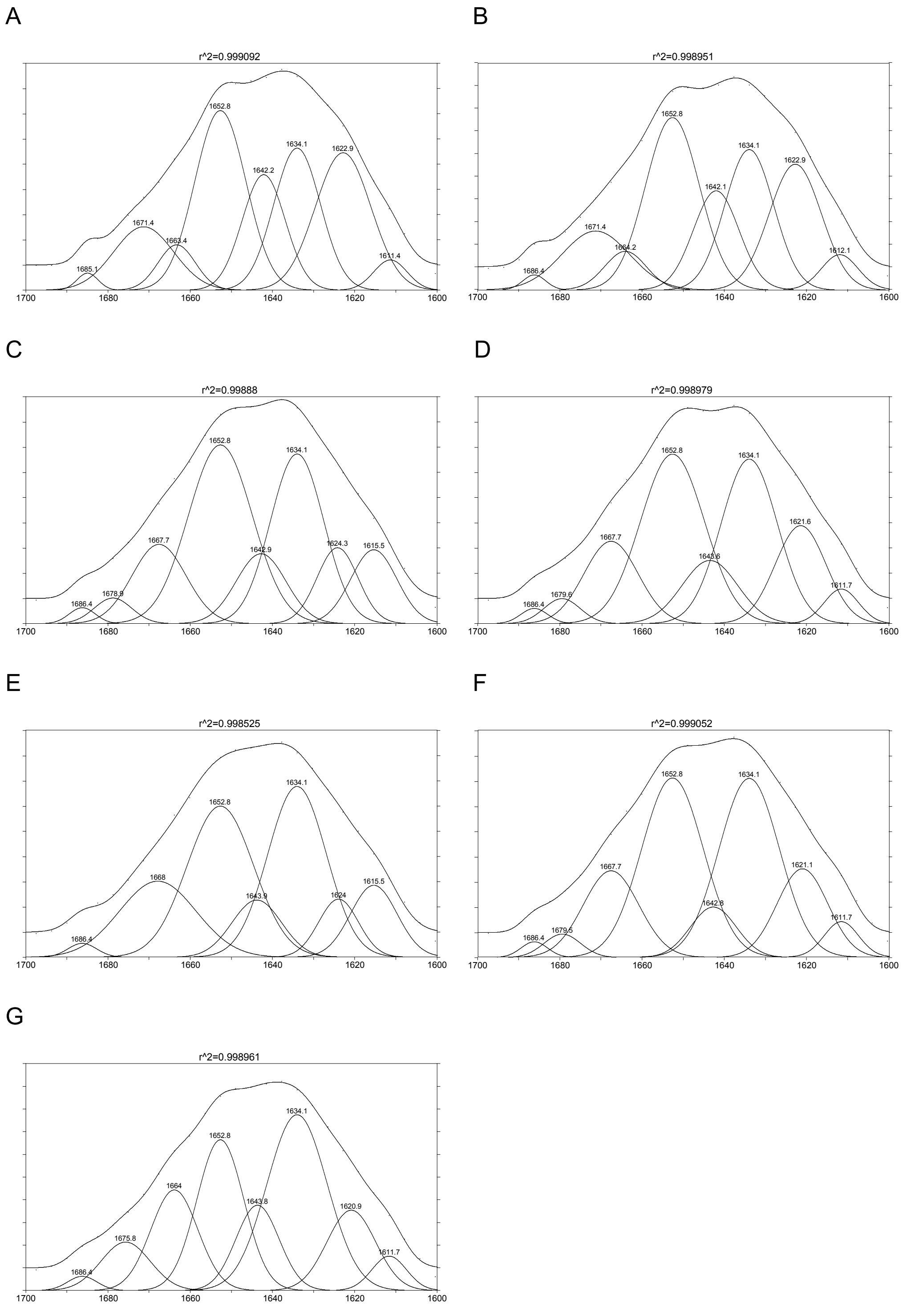

Figure A3. Secondary derivative FTIR spectrum under conventional heating at slow (A) and fast (B) heating rate and under microwave irradiation at different microwave power from 160 W (C), 320 W (D), 480 W (E), 640 W (F) and 800 W (G).

Table A3. Infrared band positions, band areas determined by curve fitting, and band assignments in the amide I spectral region of BSA under conventional heating at slow and fast heating rate and under microwave irradiation at different microwave power.

Sample	Band position (cm^{-1})	Percentage of band area (%)	Band Assignment
Slow conventional heating	1611	2.9 ± 0.06	β-Sheet
	1623	21.7 ± 0.5	β-Sheet
	1634	18.7 ± 0.3	β-Sheet
	1642	14.1 ± 0.3	Random coil
	1653	26.0 ± 0.7	α-Helix
	1663	4.8 ± 0.07	β-Turn
	1671	10.8 ± 0.1	β-Turn
	1685	1.0 ± 0.04	β-Turn
Fast conventional heating	1612	3.7 ± 0.08	β-Sheet
	1623	19.1 ± 0.2	β-Sheet
	1634	19.9 ± 0.6	β-Sheet
	1642	13.1 ± 0.3	Random coil
	1653	27.0 ± 0.5	α-Helix
	1664	4.7 ± 0.05	β-Turn
	1671	11.5 ± 0.2	β-Turn
	1686	1.0 ± 0.02	β-Turn
160 W	1615	9.4 ± 0.09	β-Sheet
	1624	8.6 ± 0.07	β-Sheet
	1634	25.0 ± 0.5	β-Sheet
	1643	9.6 ± 0.1	Random coil
	1653	31.6 ± 0.4	α-Helix
	1668	11.9 ± 0.2	β-Turn
	1679	2.7 ± 0.02	β-Turn
	1686	1.2 ± 0.03	β-Turn
320 W	1612	3.4 ± 0.06	β-Sheet
	1622	14.0 ± 0.4	β-Sheet
	1634	26.1 ± 0.6	β-Sheet
	1644	9.9 ± 0.1	Random coil
	1653	30.4 ± 0.3	α-Helix
	1668	12.6 ± 0.3	β-Turn
	1680	2.6 ± 0.2	β-Turn
	1686	1.2 ± 0.06	β-Turn
480 W	1616	9.6 ± 0.1	β-Sheet

	1624	6.7 ± 0.1	β-Sheet
	1634	28.7 ± 0.6	β-Sheet
	1644	8.2 ± 0.2	Random coil
	1653	28.9 ± 0.4	α-Helix
	1668	16.8 ± 0.3	β-Turn
	1686	1.2 ± 0.03	β-Turn
640 W	1612	3.4 ± 0.05	β-Sheet
	1621	12.5 ± 0.2	β-Sheet
	1634	30.0 ± 0.6	β-Sheet
	1643	6.4 ± 0.4	Random coil
	1653	30.7 ± 0.5	α-Helix
	1668	13.4 ± 0.7	β-Turn
	1680	2.4 ± 0.08	β-Turn
	1686	1.2 ± 0.1	β-Turn
800 W	1612	3.5 ± 0.08	β-Sheet
	1621	11.5 ± 0.4	β-Sheet
	1634	31.2 ± 0.7	β-Sheet
	1644	10.8 ± 0.2	Random coil
	1653	20.8 ± 0.7	α-Helix
	1664	13.9 ± 0.3	β-Turn
	1676	7.0 ± 0.3	β-Turn
	1686	1.2 ± 0.1	β-Turn